Int. J. Renew. Energy Dev. 2026, 15 (5), 1063-1074



Contents list available at IJRED website

**International Journal of Renewable Energy Development**

Journal homepage: https://ijred.undip.ac.id

Research Article

# Economic environmental optimization in multiple renewable energy sources with demand response based on multi-objective optimization algorithm

Zhifeng Li[a] and Shuang Zhang[b*]

[a] *School of Chemical Process Automation, Shenyang University of Technology, ShenYang 110000, LiaoNing, China*

[b] *College of Business and Trade, Shenyang University of Technology, ShenYang 110000, LiaoNing, China*

**Abstract**. The use of renewable energy sources in distribution networks results in considerable environmental and economic benefits, but it introduces challenges related to uncertainty, intermittency, and system stability. A complete multi-objective optimization model is developed that integrates renewable energy units, battery energy storage systems, electric vehicles, demand response programs, and hydro turbine units to solve these problems. The proposed methodology achieves cost savings and reduces carbon footprint while maintaining operational stability in the system. The optimization model includes full mathematical representations of all components including photovoltaic and wind generation systems and battery energy storage system state-of-charge dynamics and electric vehicle charging and discharging schedules and controllable hydro generation. A time-of-use demand response scheme is adopted to model demand flexibility which allows for load shifting and increased renewable utilization. The model is employed in a case study of 150 customers; the framework shows its efficiency through comparative simulations that evaluate performance under scenarios with demand response and without demand response. The results show that demand response reduces peak demand, improves storage coordination, and increases renewable integration. The demand response lowered costs to $6,300-$11,150 and emissions to 12,825-12,860 kg. The configuration of electrical vehicle and battery energy storage systems are combined to achieve peak shaving allowing customers to support the grid and the hydro turbine can provide effective back up power when the renewables are unavailable. The results indicate that coordinated optimization of renewables with storage and demand flexibility leads to improvements in cost-emission performance while enhancing sustainability and system resiliency.

**Keywords:** Battery Energy Storage System, Demand Response, Electric Vehicle, Hydro Turbine, Multi-Objective Optimization, Renewable Energy Source.



Received: 14th November 2025; Revised: 26th Feb 2026; Accepted: 28th May 2026; Available online: 5th August 2026

## 1. Introduction

The transition toward RES promises advancements in the global energy landscape, bringing into focus issues such as energy security, reduced adverse environmental impacts, and curtailment of dependence on fossil fuel sources (Holechek *et al.,* 2022; Rabbi *et al.,* 2022). However, there is inherent uncertainty and intermittency in RES, which pose challenges to system stability, reliability and economic operation (Islam *et al.,* 2024; Munnaf *et al.,* 2024). BESS, DR, EVs and hydro systems are among the technologies that have arisen in response to these challenges (Saldarini *et al.,* 2023; Vanlalchhuanawmi *et al.,* 2024). These technologies not only provide operational flexibility, but also enable peak shaving, load shifting and economical utilization of surplus renewables (Hojjatinia *et al.,* 2024).

In this context, MOO frameworks have evolved into decision-support tools that can balance the potentially conflicting objectives of cutting costs, reducing emissions, and maintaining the system's reliability (Behera *et al.,* 2025; Cerda-Flores *et al.,* 2022). Prior studies have employed various techniques such as mixed-integer linear programming, probabilistic modeling, and metaheuristic algorithms like grey wolf optimization and Particle Swarm Optimization (PSO) (Ahmadi *et al.,* 2022; Makhadmeh *et al.,* 2023). These approaches have shown notable improvements in operational performance; nonetheless, additional advancement requires a more comprehensive co-optimization of diverse resources inside a cohesive framework, covering PV systems, wind turbines, battery energy storage systems, electric vehicles, demand response programs, and hydro turbine technologies. (Khalil *et al.,* 2024; Ochoa-Correa *et al.,* 2025).

The various functions of DR combined with the storage flexibility provided by EVs and BESS, provide significant potential for system efficiencies and system resilience. Additionally, hydro turbine unit can bring stability, e.g., by providing backup power, and can also help mitigate intermittency when coupled with RES. The integration of these heterogeneous elements into a comprehensive optimization framework creates the opportunity to reduce costs and

* Corresponding author:
Email: woshi2tc@163.com (S. Zhang)

https://doi.org/10.61435/ijred.2026.61951
ISSN: 2252-4940/© 2026.The Author(s). Published by CBIORE

emissions while developing resilient, sustainable and intelligent energy systems suitable for modern DN.

Taha *et al.* (Taha *et al.,* 2022) demonstrated the MOO planning model to optimize the integration of RES-based DG, DR, BESS, capacitor banks, and renewable energy curtailment inside a DN. The planning model identified optimal locations and capacities of RES-DG, DR, BESSs, capacitor banks, as well as optimal curtailment of RES generation to maximize economic benefits subject to pre-determined constraints of voltage stability and power losses. These integration measures ultimately resulted in reduced variability of renewable resources, reactive power limits and power quality issues. The MOO planning model was coded and tested in the GAMS environment utilizing the IEEE 33-bus radial distribution system, demonstrating the viability of coordinated optimization to achieve techno-economic benefits. Ebrahimi and Abedini (Ebrahimi *et al.,* 2022) investigated the peak load shifting problem in smart grids via DR programs. They modeled load-shifting as a MOO problem aimed at minimizing cost for a customer, the peak demand and losses, and improving voltage stability. Simulations using the Simplex with the CPLEX solver in GAMS and Improved Grey Wolf Optimization (IGWO) in MATLAB showed that CPLEX was more effective than IGWO in reducing peak load and production cost for residential, commercial and industrial microgrids. CPLEX lowered peak load by 6.7%, 1%, and 16%, and costs by 3.5%, 2.2%, and 3.9%, respectively. Zhang *et al.* (Zhang *et al.,* 2023) investigated optimal microgrid design using energy hubs that incorporated renewable and fossil energy sources, hydrogen storage, EV, and regulated loads. The study aimed to lower power generation costs and emissions while accounting for uncertainties such as load and renewable output through probabilistic modeling. A multi-objective random algorithm applied to optimize the system. The first case study reduced operational costs by 20.75% and 15.17% compared with the second and third cases, while simultaneously reducing environmental pollution by 7.94% and 2.23%, respectively. Cicek (Çiçek, 2023) used mixed-integer linear programming to develop a multi-objective stochastic energy management model for hydrogen-based community supported by renewables. The model combines a hydrogen energy system with an electrolyzer, hydrogen tank and power cell to provide electricity for the community in addition to fuel for fuel-cell EV. A DR program facilitates the remote regulation of residential temperature settings, concurrently enabling the procurement of electricity from the power grid and the exchange of hydrogen with the primary hydrogen network. The model additionally incorporates considerations of renewable energy curtailment and the associated costs of carbon emissions. Case studies utilizing actual data from Spain showed that the proposed method reduced community costs by 58.67%. Alzahrani *et al.* (Alzahrani *et al.,* 2023) developed a multi-objective energy optimization model for smart power grids to reduce uncertainty and reconcile conflicting parameters in generation and demand. The model minimized operational costs and emissions by using RES (solar and wind) and employed a probability density function to address generation uncertainty. The multi-objective wind-driven optimization algorithm was evaluated in comparison with the multi-objective PSO algorithm. Findings indicated that algorithm decreased operational costs about 11.91% and pollution emissions by 6.12%, outperforming other models. Karimi *et al.* (Karimi *et al.,* 2023) examined a methodology for multi-energy microgrid systems scheduling with the technology, economic, and environmental objectives. With this method, the steam heating, electrical, water sectors, and cooling are merged, thus giving microgrids more flexibility and reliability. A multi-layer scheduling technique is mainly concerned with the reduction of carbon emissions, operational costs, the enhancement of system independence, and groundwater extraction. In the first layer, cost-effective operation management is prioritized; in the second layer, environmental and social aspects are addressed by reducing groundwater extraction and pollution; in the third layer, the microgrid system efficiency, voltage profile, power losses, and power quality are improved to improve system independence. When the case study is applied, the improvement of 22.81% in system independence, and 17.59% in power losses, are achieved. Jia *et al.* (Jia *et al.,* 2024) investigated a regional energy system incorporating energy storage, renewable energy, and power and thermal flows among stations. They considered a multi-objective model that minimizes cost, carbon footprint, and improves reliability. The authors analyzed the system advantages (inter-station energy exchange + local storage). The results indicated the superiority of the proposed system over others regarding energy saving, carbon emission, autonomy, costing, energy demand, carbon emissions, and power interaction, having an annual cost of 38.41 CNY/m², primary energy demand of 16.26 kWh/m², carbon emissions of 4.33 kg/m², and power interaction of 9.99 kWh/m², contributing to the theoretical foundation for the development of regional loLES. A modified Golden Jackal Optimization algorithm, named Enhanced Golden Jackal Optimization (GJO), was suggested by Kumar and Karthikeyan in (Kumar *et al.*, 2024) The proposed technique was applicable within the realm of BESSs and hybrid energy production management. The proposed technique addressed the aspects of minimized operational cost, sustainability of microgrid energy management, and other constraints such as balancing the power equation, production capability, consumer demand, and dynamic behavior of the storage devices. The proposed algorithm was compared to the existing techniques of PSO and artificial bee colony algorithms. The findings indicated that GJO achieved 96% increase in efficiency and a cost reduction of $\$2{\times}10^6$ relative to other methods. Ali *et al.* (Ali *et al.,* 2024) suggested an approach for optimizing the integration of hydrogen systems and DR in smart grids to increase the hosting capacity of RES. The coordinated management system includes hydrogen tanks, fuel cells, hydrogen load DR, RES curtailment, storage charging rates, and EV flexibility with G2V/V2G capabilities. The MOO model aims to decrease costs while increasing HC. Simulation findings indicated a 17.24% increase in Hosting Capacity (HC) and a significant cost decrease, in addition to the appropriate number of Hydrogen Storage (HS) to maximize RES capacity.

Despite these efforts, several gaps remain, although studies have been conducted on the incorporation of energy storage systems, renewable energy, and disaster recovery within DN, most previous studies have had a narrow focus: either purely economic performance, environmental impact, or a single technology in isolation. For instance, some studies emphasize minimizing cost while disregarding emissions, while other works stress the importance of high renewable penetration without considering the combined impact of flexible DR and controllable hydro turbine (HT) units as system-support resources. Moreover, few optimization models consider the integrated contribution of PV, wind, BESSs, EVs, DR, and HT within a holistic framework. Consequently, comprehensive models that address cost, emission, renewable variability, and system reliability under different DR scenarios are still limited.

To clearly position this work within the existing literature to address the above gaps, the main contributions are summarized that the study provides complete MOO framework for DN operation that includes PV systems, wind turbines, BESS, EVs, DR programs and HT unit. As opposed to alternative methodologies, the configuration integrates a joint management strategy to incorporate DR for load shifting methods, EV operation to function as flexible distributed storage, and HT as controllable generation to enhance reliability. The system jointly optimizes economic and environmental objectives over the same scheduling horizon while generating clear Pareto fronts, allowing decision-makers to evaluate trade-offs when lowering costs and reducing emissions levels. Notably, this configuration emphasizes DR's role in increasing renewable energy consumption levels while reducing imported grid energy, thereby supporting sustainability at both the individual-user and aggregated levels. Ultimately, this comprehensive strategy contributes to literature by connecting studies that have been solely technology-based with the contemporary need for low-carbon, resilient energy systems in practice.

## 2. Methodology

The methodology develops reliable MOO framework for DN for minimize the operational costs and emissions. The system integrates PV WT, BESS, EVs with vehicle-to-grid capability, DR and HT unit as a controllable resource. Each equipment model with related mathematical formulations and constraints including power balance, generator limits, SOC boundaries, and hydro-resource availability is represented in subsections of section 2. A Pareto-based optimization algorithm (NSGAII) is used to minimize economic and environmental objectives simultaneously. The framework is substantiated through a rigorous validation process of a 24-hour case study involving 150 users, capturing hourly demand, imported energy prices, renewable generation, and storage interactions under scenarios with and without DR participation. The optimal energy management system for microgrids is presented in Fig. 1. Scalability beyond the 150-user case study is discussed by noting that the computational burden of NSGA-II increases with the chosen population size and number of generations, and more critically in the present framework with the cost of evaluating each candidate schedule. For each candidate solution, objective values and feasibility checks are computed across the full 24-hour horizon and across all users and modeled, including operational constraints such as power balance and device limits. As the number of users and/or modeled resources increases, the per-candidate evaluation workload increases accordingly under fixed NSGA-II settings, resulting in higher overall runtime.

### *2.1. PV model*

The power production of a PV array depends on solar irradiance incident on the roof surface, the ambient temperature, and the PV module characteristics. The widely used physical representation is presented in Eq. (1) (He et al., 2022; Lahlou et al., 2023).

$$P_{\mathrm{PV}} = P_{\mathrm{PV}}^{\mathrm{rated}} \times \frac{I_{\mathrm{T}}}{I_{\mathrm{ST}}} \times \left[1 - \beta \times \left(T_{\mathrm{amb}} + (\mathrm{NOCT} - T_{\mathrm{re}}) \times \frac{I_{\mathrm{T}}}{I_{\mathrm{ref}}} - T_{\mathrm{ST}}\right)\right] \tag{1}$$

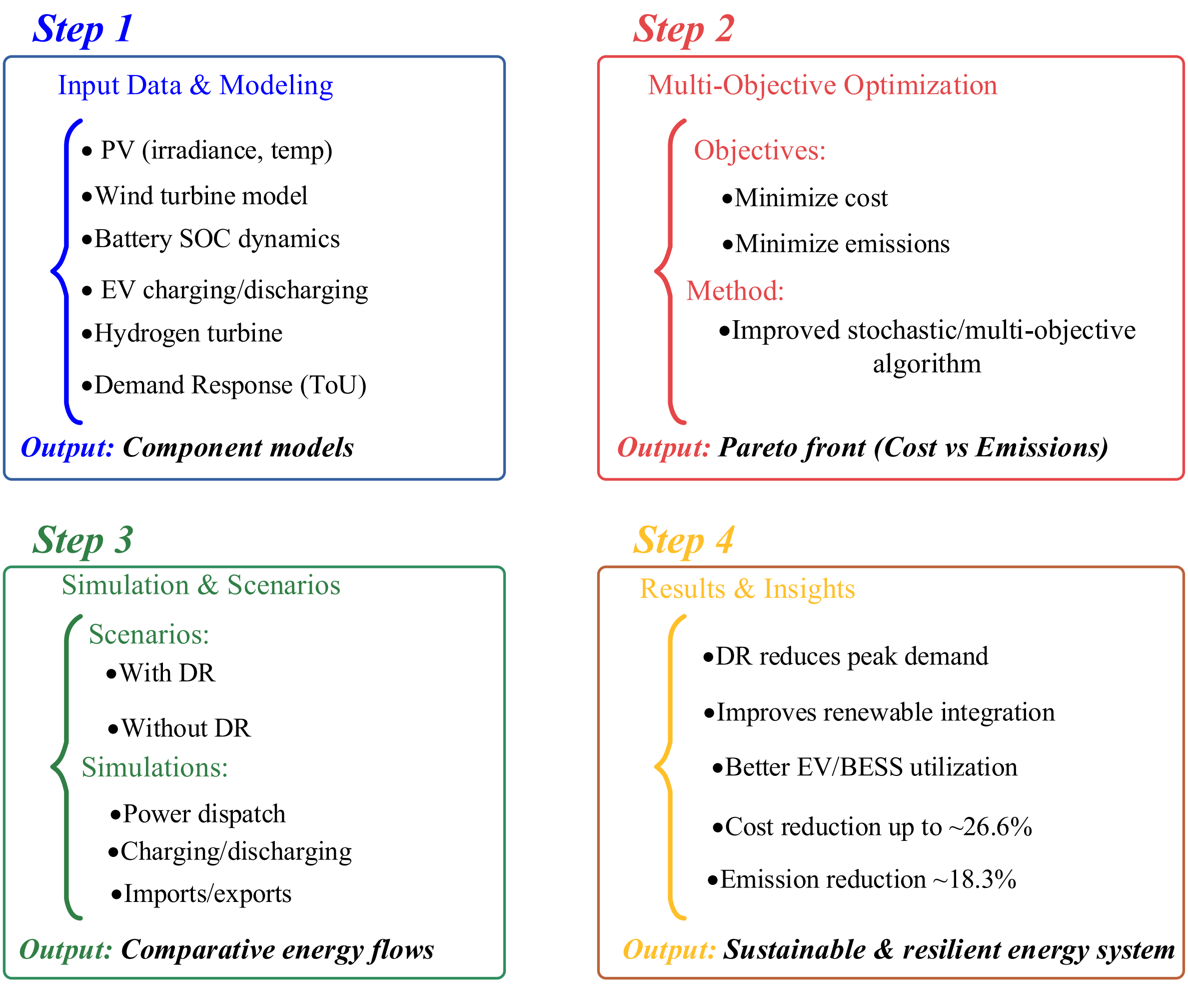


**Fig. 1.** The Proposed Optimal energy management system for the proposed MG.

The variables $P_{\mathrm{PV}}$ and $P_{\mathrm{PV}}^{\mathrm{rated}}$ represent the real power produced and rated power output of the PV array, respectively. $I_{\mathrm{T}}, I_{\mathrm{ST}}$, and $I_{\mathrm{re}}$ represent the real, Standard Test Condition (STC), and base solar irradiance, respectively. $T_{\mathrm{amb}}$ denotes the ambient temperature, β denotes the temperature coefficient, and NOCT stands for nominal operating cell temperature.

### 2.2. Wind turbine model

The optimal model must be applied to compute the wind turbine power output. Eq. (2) is usually used to determine generated power by a wind turbine as follows (Güven et al., 2023; H. Zhang, 2024).

$$P_{WT}=\begin{cases}0 \; v(t)\leq v_{\text{c-in}} \quad \text{Or} \quad v(t)\geq v_{\text{c-out}}\\ P_r\times\dfrac{v(t)-v_{\text{c-in}}}{v_r-v_{\text{c-in}}} \; v_{\text{c-in}}\leq v(t)\leq v_r\\ P_r \; v_r\leq v(t)\leq v_{\text{c-out}}\end{cases} \tag{2}$$

The subsequent parameters belong to the wind turbine, $P_r$( kW) denotes the nominal power, with the subsequent speed characteristics $v(t)(\mathrm{m/s})$ .Wind speed is often recorded at a specific elevation, and the wind speeds at different altitudes can be estimated using the power factor $a_h$ in Eq. (3) as follows (Güven et al., 2023):

$$V_t=V_m*\left(\frac{H_t}{H_m}\right)^{a_h} \tag{3}$$

$H_t$ denotes wind turbine hub height, $\mathrm{H_m}$ denotes the base height, $V_m$( m/s) signifies the base wind speed quantified at ,$V_t$(m/s) represent the wind speed at the hubs level, whereas $a_h$ signifies exponential power law's factor. The $a_h$ is based on the geography and climatic environment of the location and typically ranges between 0.05 and 0.5.

### 2.3. BESS

The battery with lithium-ion cells is chosen as energy storage system. The State of Charge (SOC) of battery storage can be represented as stated in Eq. (4) (Y. Zhang *et al.,* 2020):

$$SOC(i+1)=SOC(i)+\frac{P_{\mathrm{ch}}(i)t_{\mathrm{ch}}(i)\eta_{\mathrm{ch}}}{E_{\mathrm{usa}}}-\frac{P_{\mathrm{dis}}(i)t_{\mathrm{dis}}(i)}{E_{\mathrm{usa}}\eta_{\mathrm{dis}}}-\frac{P_{\mathrm{sf-dis}}(i)}{E_{\mathrm{usa}}} \tag{4}$$

$SOC$ denotes the SOC of the battery (%), $E_{usa}$ signifies the usable battery energy capacity over a whole cycle (kWh), and $i$ signifies the time iteration for nearly all parameters. $P_{ch}$ denotes the battery charging power, $t_{ch}$ represents the rechargeable batteries charging period, assumed to be a value of one or zero, $\eta_{ch}$ indicates the battery charging efficiency, $P_{dis}$ signifies the battery discharging power, $t_{\mathrm{dis}}$ refers to the battery discharge period, also assumed to be a value of 1 or 0, $\eta_{\mathrm{dis}}$ denotes the battery discharge efficiency, and $P_{sf-dis}$ represents the battery self-discharging power. The battery is incapable of undergoing charging and discharging processes concurrently; therefore, the durations for both processes are constrained as follows (Kheiter *et al.,* 2022; Yu *et al.,* 2024; Y. Zhang *et al.,* 2020):

$$\mathrm{t_{ch}}(i)+t_{\mathrm{dis}}(i)\leqslant t_{\mathrm{step}} \tag{5}$$

To ensure that the charging and discharging of the battery only occur during the time period that has been stated in the proposed model, two binary availability indicators are introduced, let $t\in\{1,\ldots,24\}$ denote the hourly time slot with $\Delta t=1h$. The charging and discharging availability indicators are defined as:

$$t_{\mathrm{ch}}(i)=\begin{cases}1, & \text{if } 9\leq i\leq 16\\ 0, & \text{otherwise}\end{cases} \tag{6}$$

$$t_{\mathrm{dis}}(i)=\begin{cases}1, & \text{if } 17\leq i\leq 22\\ 0, & \text{otherwise}\end{cases} \tag{7}$$

where $\mathrm{t_{ch}(t)}\in\{0,1\}$ and $\mathrm{t_{dis}(t)}\in\{0,1\}$ signifies whether charging and discharging is permitted at hour t respectively. So, charging is allowed during hours 9–6 and discharging during hours 17–22 of the 24-hour scheduling horizon.

The SOC should stay within the min and max limits during entire simulation (Qachchachi *et al.*, 2020):

$$SOC_{\min}\leqslant SOC(i)\leqslant SOC_{\max} \tag{8}$$

where $SOC_{\min}$ denotes the min limit and $SOC_{\max}$ denotes the max limit of $SOC$. It is determined to be 0.2 the lower limit and 1 the upper limit.

### 2.4. EV

The area of parking is presumed to have knowledge of the arrival and departure times of all EV. The accessible electricity of EV at the station $i$ for the site of parking is delineated in Eq. (9). Before the EV's arrives and after it leaves, the energy available to the charging ports to which the vehicle is connected is zero. When the EV arrives at the charging facility, the energy at port $i$ is called initial energy $E_i^{ini}$. During the time that the vehicle is parked, the energy changes based on the energy provided in the past time interval and the current charging/discharging activity. Finally, before the EV departs from the parking facility, the EV achieves its upper limit of energy which is usually less than 100% of the total battery capacity in order to safely avoid overcharging as seen in Eq. (10), below. Eqs. (11) and (12) introduce the binary variable $\mu_{i,t,s}$ which guarantees the EV cannot simultaneously charge and discharge. Energy levels for the EV are constrained in Eq. (13) with the lower limit denoted as $E_{i,\min}^{EV}$ and the upper limit as $E_{i,\max}^{EV}$. In addition, Eq. (14) establishes that it is not possible to charge or discharge the EV if there is not an EV located at the charging facility (Qi et al., 2023).

$$E_{i,t,s}^{EV}=\begin{cases}0, & t<t_{a,i}\\ E_i^{ini}, & t=t_{a,i}\\ E_{i,t-1,s}^{EV}+\left(\eta_{ch}*P_{i,t,s}^{EV+}-\dfrac{1}{\eta_{dis}}*P_{i,t,s}^{EV-}\right)\Delta t, & t_{a,i}<t\leq t_{d,i}\\ E_{i,max}^{EV} & t=t_{d,i}\\ 0 & t>t_{d,i}\end{cases} \tag{9}$$

$$E_{i,\max}^{EV}=E_i^{initial}+\sum_{t=t_{a,i}+1}^{t_{d,i}}\left(\eta_{ch}^{EV}*P_{i,t,s}^{EV+}-\frac{1}{\eta_{dis}^{EV}}*P_{i,t,s}^{EV-}\right)\Delta t \tag{10}$$

For $t_{a,i}<t\leq t_{d,i}$,

$$0\leq P_{i,t,s}^{EV+}\leq\mu_{i,t,s}*P_{i,\max}^{EV+} \tag{11}$$

$$0\leq P_{i,t,s}^{EV-}\leq(1-\mu_{i,t,s})*P_{i,\max}^{EV-} \tag{12}$$

$$E_{i,\min}^{EV}\leq E_{i,t,s}^{EV}\leq E_{i,\max}^{EV} \tag{13}$$

For $t$ otherwise

$$P_{i,t,s}^{EV+} = P_{i,t,s}^{EV-} = 0 \tag{14}$$

In scenario $s$, the available energy of the EV at station $i$ for the parking lot to utilize at time $t$ is denoted as $E_{i,t,s}^{EV}$. The time it takes for the EV to arrival and departure is represented by $t_{a,i}$ and $t_{d,i}$, the power required to charge and discharge the vehicle is $P_{i,t,s}^{EV+}$and $P_{i,t,s}^{EV-}$, the efficiency of charging and discharging is $\eta_{ch}^{EV}$ and $\eta_{\mathrm{dis}}^{EV}$, respectively, and the time period is $\Delta t$. The maximum power for charging and discharging EV are signified by $P_{i,\max}^{EV_+}$and $P_{i,\max}^{EV-}$, respectively.

### 2.5. Demand Response

In Distribution Networks (DN), it is essential to control load flexibility to optimize energy consumption and ensure well-organized operation. The DR notably improves the efficacy of the DNs. This research proposes a fully-fledged DR model through a ToU method that enables load in the DN to serve as a DR resource and facilitate real-time interaction and coordination between the different sources of energy. The DR formulation is defined in Eqs. (15-17) (Duan *et al.*, 2025; Saeed *et al.*, 2023):

$$P_{DR}^{t} = \left[\mathrm{Load}_{\mathrm{base}}^{t} - \mathrm{Load}_{DR}^{t}\right] \cdot \Delta t; \forall t \in T \tag{15}$$

$$\mathrm{Load}_{DR}^{t} = \left[\mathrm{DR}_{t} \times \mathrm{Load}_{\mathrm{base}}^{t}\right] \cdot \Delta t \,; \forall t \in T \tag{16}$$

$$0 \leq DR_t \leq 1\,; \forall t \in T \tag{17}$$

$P_{DR}^{t}$ denotes the power of DR at time t, $DR_t$ is shift of DR.

### 2.6. Hydro Turbine

The HT is modeled as a controllable hydropower unit that provides scheduled generation within technical constraints. Hydro operation is represented using a capacity bound and an equivalent available hydro-energy (water-budget) constraint to prevent over-dispatch over the 24-h horizon. The HT output power at time $t$ is limited by Eq. (18) as follows (Han *et al.,* 2024):

$$0 \leq P_t^{HT} \leq P^{HT(\max)} \tag{18}$$

Hydro generation over the horizon is limited by the available hydro energy as follows in Eq. (19):

$$\sum_t P_t^{HT} \Delta t \leq E_{HT}^{avail} \tag{19}$$

where $\mathrm{E}_{\mathrm{HT}}^{\mathrm{avail}}$(kWh) signifies the available hydro energy over the scheduling horizon. This energy can be related to the available water resource through an equivalent conversion.

$$E_{HT}^{avail} = \kappa_{HT} w_{avail} \tag{20}$$

where $W_{avail}$ represents the usable water volume over the horizon and $\kappa_{HT}$ is an equivalent conversion coefficient that captures effective head and turbine-generator efficiency. This formulation ensures feasible HT scheduling without requiring a detailed hydraulic model.

### 2.7. Objectives

#### 2.7.1. Economic objective (Total cost minimization)

The total cost over the scheduling horizon is given as:

$$\mathrm{Cost} = \sum_{t=1}^{T} \left(C_t^{\mathrm{grid\_buy}} \cdot P_t^{\mathrm{grid\_buy}} + C^{HT} \cdot P_t^{HT} + C_t^{DR} \cdot P_t^{DR} + C^{EV_{Ch}} \cdot P_t^{EV_{Ch}} + C^{EV_{Dch}} \cdot P_t^{EV_{Dch}} + C^{batt_{Ch}} \cdot P_t^{batt_{Ch}} + C^{batt_{Dch}} \cdot P_t^{batt_{Dch}} + C^{\mathrm{grid\_sell}} \cdot P_t^{\mathrm{grid\_sell}}\right) \tag{21}$$

where $C_t^{\mathrm{grid}}$ signifies the price of the electricity at time $t$, $P_t^{\mathrm{grid}}$ represents the imported power from grid, $C^{HT}$ denotes the denotes the hydro turbine marginal operating cost coefficient, and $C_t^{DR}$ represents the cost (or incentive payment) associated with DR adjustments.

These objective captures both direct energy costs and DR-related costs, while providing economic incentives to use renewables and storage optimally.

#### 2.7.2. Environmental objective (Emission minimization)

The total emissions are calculated as:

$$\mathrm{Emission} = \sum_{t=1}^{T} \left(EF^{\mathrm{grid}} \cdot P_t^{\mathrm{grid}} + EF^{HT} \cdot P_t^{HT}\right) \tag{22}$$

where $EF^{\mathrm{grid}}$ is the emission factors ( kg/kWh ) associated with grid electricity. For renewables (solar, wind), storage (BESS, EV), and HT emission contributions are considered negligible.

#### 2.7.3. Multi-Objective formulation

The two objectives are optimized simultaneously: $\min\{\mathrm{Cost}, \mathrm{Emission}\}$, subject to operational, technical, and storage constraints defined in the system model (PV, wind, BESS, EV, HT, and DR). A Pareto front is obtained, enabling trade off analysis between cost and environmental performance.

## 3. Results and discussion

This section provides the simulation outcomes of the suggested MOO model, examining the system's performance under scenarios with and without DR to evaluate cost, emissions, and resource utilization outcomes.

### 3.1. Input analysis

#### 3.1.1. Price input

Fig. 2a shows the 24-hour TOU electricity price used in the cost objective. The profile includes a distinct peak-price period (17:00–21:00) and lower off-peak prices earlier in the day, establishing the price variation that the day-ahead optimization accounts for when scheduling grid exchange and flexibility resources under their constraints.

#### 3.1.2. Demand profile for users and general profile

Fig. 2b reports the demand inputs across the 150 users (user-indexed energy demand), capturing load heterogeneity in the case study. These inputs are held fixed across scenarios; in the DR case, demand is modified only through the bounded DR formulation, so subsequent differences in dispatch and cost-emission outcomes are attributable to DR-enabled flexibility rather than changes in the underlying demand data.

Fig. 3a documents the two demand inputs used for the single-user case: the baseline demand and the DR-adjusted demand generated only through the bounded DR formulation. These profiles are then scheduled using the same 24-h EMS model, ensuring the subsequent differences between scenarios are attributable to DR-enabled flexibility under unchanged underlying data.

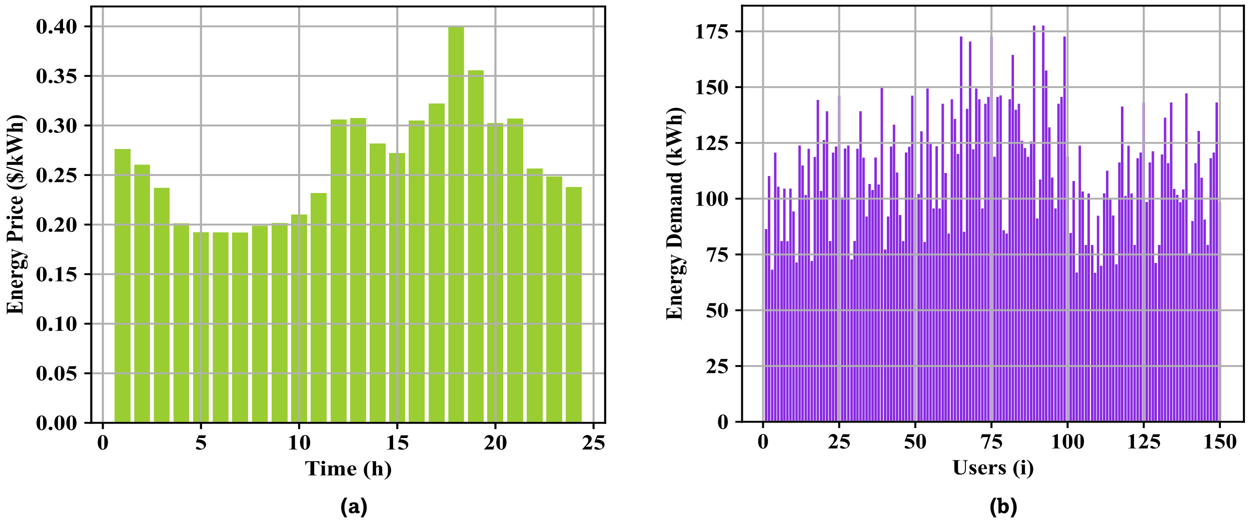


**Fig. 2.** 24-hour TOU electricity price (a), Demand inputs (b).

Fig. 3b presents the community-level demand used in the 24-h EMS, comparing the baseline aggregate load with the DR-adjusted aggregate load obtained by applying the bounded DR formulation. The baseline profile exhibits a stronger peak tendency, whereas enabling DR yields a more distributed aggregate requirement with a lower peak magnitude. Since the underlying demand inputs are unchanged across scenarios, any subsequent differences in grid exchange and cost–emission performance can be attributed to DR-enabled demand adjustment under the same EMS constraints rather than to changes in the dataset.

*3.1.3. Renewable energy inputs*

Fig. 3c reports the exogenous wind and PV generation profiles used as inputs to the 24-h EMS. The profiles indicate complementary availability over the day: PV production is concentrated around midday and decreases in the late afternoon, while wind contribution is higher later in the day. In the proposed formulation, these trajectories define the renewable supply envelope within which the optimizer schedules grid exchange and flexibility resources (BESS/EV/DR) under their operating constraints, enabling the

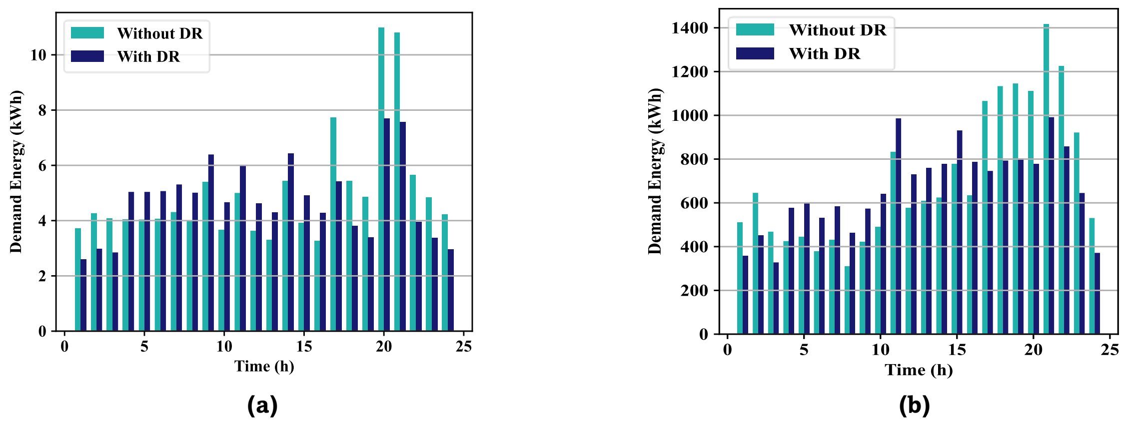


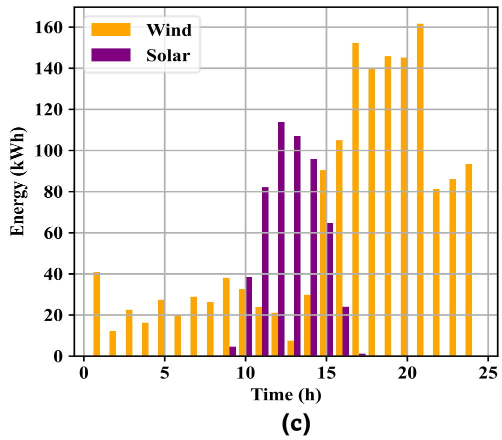


**Fig. 3.** Total demand for one user with and without DR (a), Demand profile for 150 users (b), Wind and PV inputs (c)

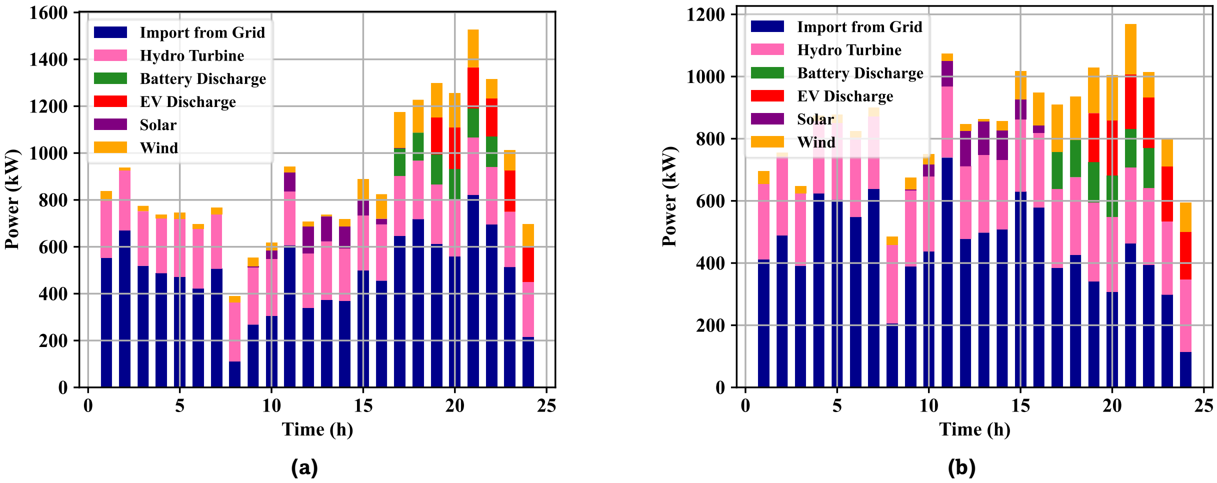


**Fig. 4.** Optimal power dispatch without DR (a) and with (b).

subsequent dispatch results to be interpreted as optimization outcomes under specified renewable availability rather than assumed operating behavior. All input profiles used in the input analysis of the electricity price(ToU), demand, and renewable generations) were obtained from: https://github.com/Energy-MAC/TSG-P2P-Pricing

*3.2. Energy management system with and without demand response*

Fig. 4 shows the optimal power dispatch across several sources, including grid import, HT, ESS, EV storage, solar and wind generation, throughout a 24-hour period for one consumer. In both cases, the system successfully combines several distributed resources to balance demand. However, major differences exist between the two scenarios. Without DR (Fig. 4a), grid import and HT provide a large share of supply, notably during the early morning and evening peak hours. Renewable participation remains low, with wind and solar contributing mostly within their availability times but not enough to reduce the reliance on imports. ESS and EV participation is low, leading to a greater reliance on conventional sources. When DR is enabled (Fig. 4b), the dispatch becomes more coordinated with renewable availability. Specifically, the model reduces reliance on expensive peak-hour grid import by shifting part of the flexible demand toward periods with higher PV/wind contribution, while BESS and EV discharging contribute more actively to support peak shaving. As a result, the required contribution from grid imports and HT during peak intervals is moderated, while maintaining overall feasibility and supply–demand

Overall, the comparison shows that DR improves system flexibility, enhances renewable utilization and reduces grid reliance. The coordinated role of ESS and EVs under DR further reduces peak demand pressures, support both economic and environmental objectives of the optimization framework. Fig. 5 presents the hourly demand, export to the grid, battery charging, and EV charging patterns across a 24-hour period, compare the scenarios without and with DR. Without DR (Fig. 5a), the system shows significant EV charging in the early morning (0-7 h), which aligns with lower energy costs and excess renewable availability. Battery charging happens intermittently between 9 and 16 hours, but with fairly small variations. Export to the grid occurs primarily during the mid-afternoon and evening, when renewable generation and storage discharge exceed local demand. However, overall system exports remain limited, indicating a strong reliance on external imports.

With the integration of DR (Fig. 5b), a more synchronized charging and export profile appears. EV charging remains concentrated during off-peak hours; but the charging energy decreases relative to the non-DR scenario, thereby aligning

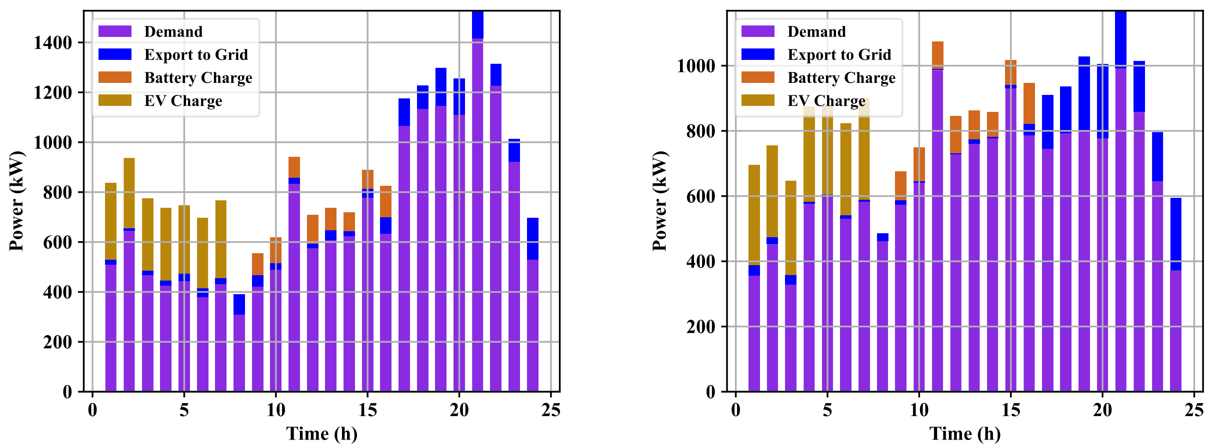


(a) Without DR (b) With DR
**Fig. 5.** Hourly charging, discharging, and export patterns under different DR scenarios.

more effectively with the available renewable energy supply. The charging rate of batteries rises particularly at midday when solar availability is greatest which allows the batteries to be discharged later during peak demand times. The grid exports are significantly higher towards the evening hours (17-24 h), indicating that excess renewable and stored energy from the batteries is exported to the network efficiently.

This comparison highlights the role of DR in shifting flexible loads to periods of renewable abundance, increasing system exports, and enhancing the overall efficiency of storage utilization. The coordinated charging of EVs and batteries under DR improves grid interaction and reduces dependency on costly peak imports.

#### 3.2.1. *Aggregate daily energy management for 150 users*

Fig. 6 shows the aggregated daily energy contribution per user for 24-hour horizon, considering 150 users in total. Each bar refers to the combined contributions of grid import, HT, ESS, EV ESS, solar and wind for one user. Without DR (Fig. 6a), most users rely on grid imports and HT, while renewables and storage acting a relatively minor role. Integration of wind and solar appears irregular and poorly aligned with overall demand, result in uneven renewable use across the user base. ESS and EV ESS contributions can be seen but not significant, resulting in a continued reliance on imports to meet daily requirements. With DR participation (Fig. 6b), the dispatch structure becomes more evenly distributed among consumers. Grid imports are significantly decreased as flexible loads shift to renewable-rich periods. ESS and EV ESS contributions are greater, supplementing solar and wind power to prepare a higher share of daily demand. Distribution of resources among users is smoother, indicating that DR improves coordination between demand and renewable availability. This comparison ensures fairer and more effective renewable energy use at the aggregated user level. By spreading the benefits of storage and demand flexibility across community, DR enhances both system efficiency and sustainability.

### 3.3. *Battery and EV charging and discharging behavior*

Fig. 7a shows hourly charge and discharge patterns of the BESS within a 24-hour timeframe. Findings distinctly emphasize the battery function in transfer energy consumption from off-peak to peak periods. From mid-morning to afternoon (about 9:00–15:00), the battery primarily operates in charging mode, with charging power ranging between 1.8 and 2.8 kW. This corresponds with times of elevated solar availability and comparatively low demand, allowing the storage of surplus renewable energy. In the evening hours (17:00–22:00), the battery shifts to discharging mode, providing up to 3 kW to the system during peak demand and pricing.

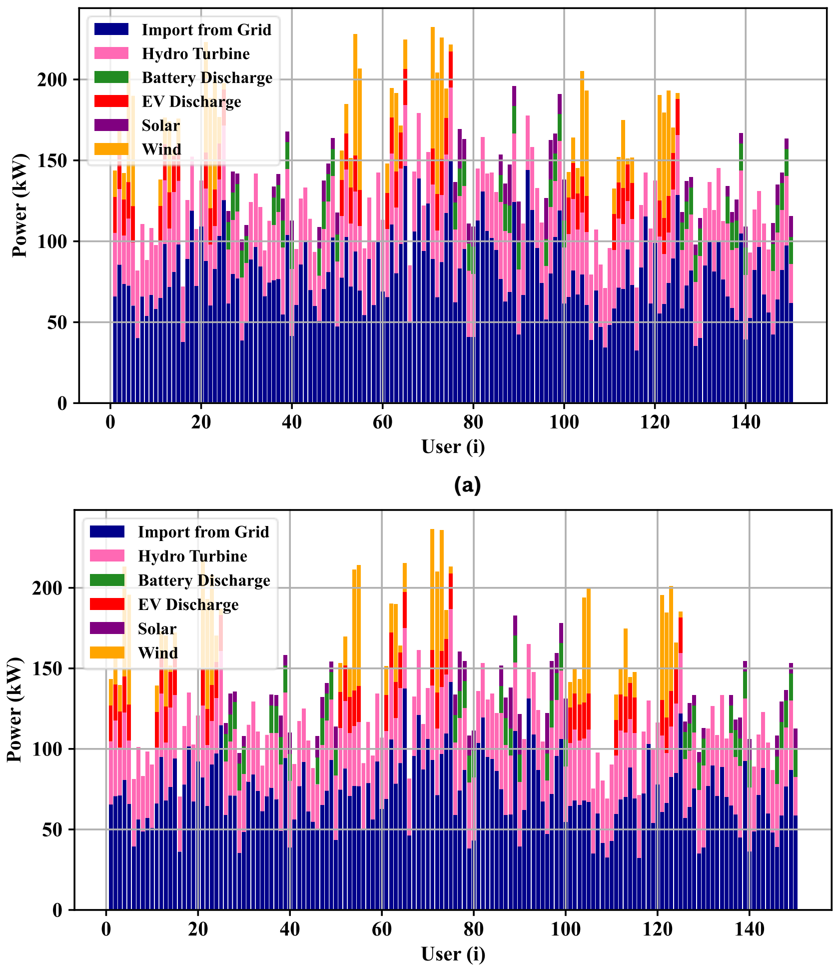


**Fig. 6.** Aggregated daily energy dispatch for 150 users without DR (a) and with (b).

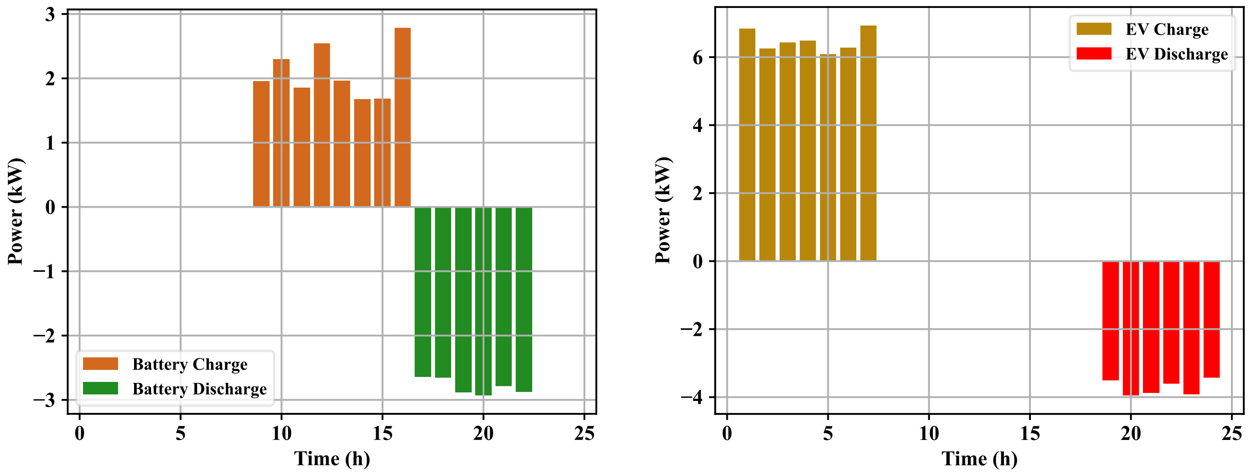


(a) (b)

**Fig. 7.** BESS and EV charge/discharge behavior.

This charge and discharge cycle shows the contribution of the battery to peak shaving and shift of demand. By absorbing surplus renewable generation and discharging during high-demand hours, the battery not only reduces reliance on grid imports but also enhances the economic and environmental performance of the system. Results confirm that storage flexibility is a critical enabler of effective renewable integration under proposed optimization model.

Fig. 7b depicts the optimized power schedule for EV charging/V2G, which is divided into two separate operation blocks. Charging is done in the early hours at 0:00-7:00 around 6-7 kW, while discharge pattern is scheduled for the evening around 19:00-24:00 at about -3.5 to -4 kW, with almost no EV power availability during the other hours. This is consistent with the ToU tariff profile, in which electricity prices are lowest in the early morning valley around 4-8 h, rise to a late-day peak, and then remain high in the evening so the optimizer shifts EV energy intake to lower-priced hours and schedules V2G export during higher-priced periods. The lower discharging magnitude compared to charging demonstrates operational limits such as V2G power bounds and minimum SOC/energy-reserve constraints, which allow peak-period support while maintaining sufficient mobility energy.

### 3.4. *Cost-Emission trade-off with and without demand response*

Fig. 8 illustrate the Pareto fronts of total cost in relation to total pollutant emissions across the two scenarios. In the absence of DR, as illustrated in Fig. 8a, system operation incurs elevated costs and emissions, with ideal solutions varying between approximately \$5,500 and \$15,200, and emissions ranging from 15,630 to 15,700 kg. The front reflects the expected trade-off: lower cost is associated with slightly higher emissions, whereas achieving lower emissions requires additional operating cost. With DR in Fig. 8b, both objectives improve simultaneously. The ideal range shifts down, with costs ranging from \$6,300 to \$11,150 and emissions reduced about 12,825-12,860 kg. When compared to the without DR scenario, the system achieves considerable decrease in operational costs and emissions, indicating the efficiency improvements from flexible demand management.

In summary, based on the results from the preceding comparison studies, the DR approach ensures improved coordination and utilization of renewable energy sources and enhances economic profitability and environmental sustainability. The best representative solution from the Pareto

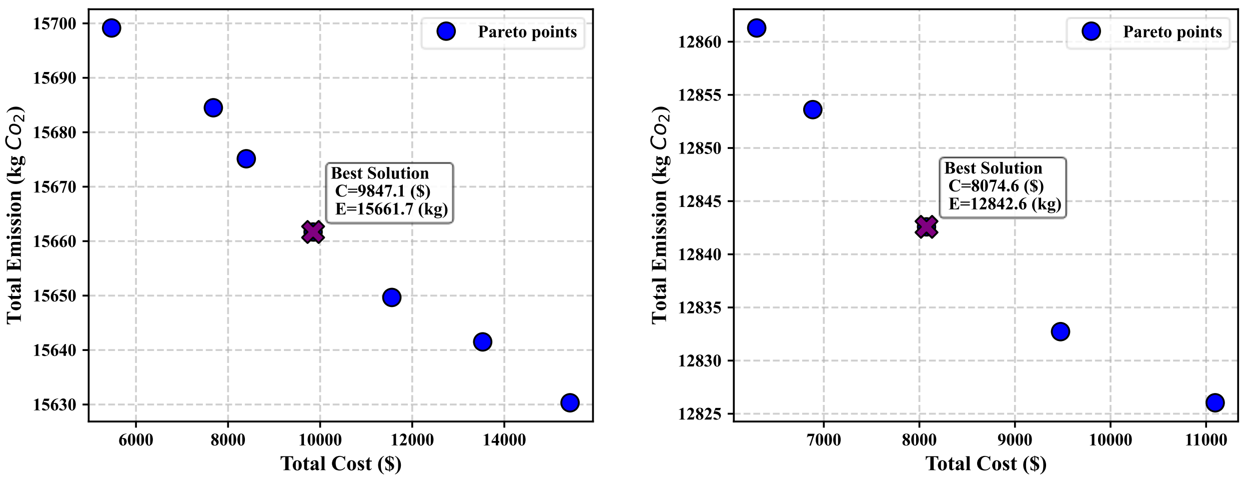


(a) (b)

**Fig. 8.** Cost and emission Pareto front without DR (a), with DR (b)

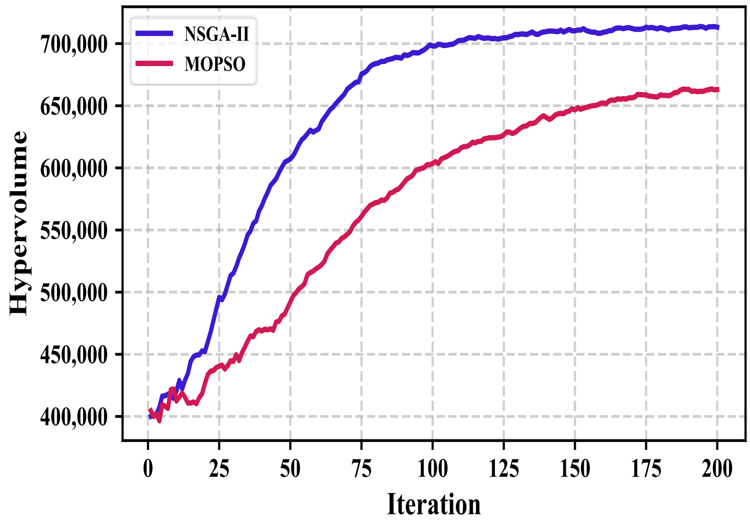


**Fig. 9.** Convergence behavior of NSGA-II and MOPSO algorithms.

**Table 1**
Results of NSGA-II and MOPSO for the best-compromise Pareto solutions.

| Algorithm | DR | Best-compromise Cost ($) | Best-compromise Emission (kg $CO_2$) | Runtime (s) |
|---|---|---|---|---|
| NSGA-II | Without | 9847.1 | 15661.7 | 342 |
| | With | 8074.6 | 12842.6 | 418 |
| MOPSO | Without | 10291.2 | 15806.3 | 354 |
| | With | 8345.5 | 13127.4 | 451 |

**Table 2**
Sensitivity of system cost, emissions, and grid exchange to hydro turbine availability.

| Hydro turbine | Cost ($) | Emission (kg) | Import From Grid (kW) |
|---|---|---|---|
| 30% | 10384.26 | 16775.12 | 14151.90 |
| 50% | 9852.76 | 15411.67 | 13164.50 |
| 100% | 8074.60 | 12842.58 | 10899.29 |

set is used in comparative analysis. Fig. 8a and Fig. 8b shows that DR improves the practical cost-emission trade-off. This is notable because DR increases performance by lowering both objectives simultaneously (without DR, C = 9847.1 and E = 15661.7; with DR, C = 8074.6 and E = 12842.6).

In measuring the success of the proposed NSGA-II solver, an analogous benchmarking of MOPSO has been conducted using the same EMS formulation and computational parameters. In this case, both algorithms are assigned a population of 50 and are set to run for 200 generations. They are also subject to the same decision-variable scope and constraints. Fig. 9 shows the convergence behavior, and Table.1 summarizes the quantitative benchmarking data.

Table 1 illustrates that in the DR case, NSGA-II achieved a better compromise by decreasing both objectives than MOPSO (NSGA-II: C = 8074.6, E = 12842.6; MOPSO: C = 8345.5, E = 13127.4), while keeping the time spent the same. Without DR, the best solutions selected show comparable NSGA-II costs C = 9847.1; MOPSO: C = 10291.2. Yet, NSGA-II attains slightly lower emissions (15661.7 vs. 15806.3). The benchmarking confirms that NSGA-II is computationally efficient, providing reliable convergence and superior cost-emission trade-offs in the examined EMS problem. As demonstrated in Table 2, a sensitivity analysis on hydro turbine availability (30%, 50%, and 100%) shows that system performance improves monotonically as hydro contribution increases. The total cost reduces from $10,384.26 (30%) to $8,074.60 (100%), emissions from 16,775.12 to 12,842.58 kg, and grid import from 14,151.90 to 10,899.29. This sensitivity analysis indicates increasing hydro turbine availability delivers more controlled supply, decreases dependence on grid purchases, and improves overall cost-emission performance.

The simulations verify the validity of the MOO approach for simultaneously optimizing costs, emissions, and the level of system reliability for the studied renewable energy management scenario. The results also highlight the importance of the variables of demand flexibility, energy storage, and coordination and optimization for achieving economically and environmentally sustainable operation.

The proposed framework provides a realistic implementation pathway for the utilities and grid operators to integrate renewables effectively within their grid and achieves the cost savings. The successful implementation of DR, EVs, and battery storage solutions at the grid level ensures the utilization of available hours where renewable resources are abundant, thus contributing to the stability of the grid. Additionally, the inclusion of the HT provides a controllable backup supply during periods of low renewable generation, complementing DR and storage flexibility and improving operational reliability.

## 4. Conclusion

This research proposes a MOO framework that incorporates PV systems, WT systems, EV resources, BESS, DR programs, and HT to improve both cost and environmental sustainability in distribution networks. The framework incorporates generalized mathematical models that describe the operation of each of the component, and then uses a Time-of-Use DR strategy to improve load flexibility can be improved. The study verified the benefits of the synchronous optimization analysis of 150 different users for a 24-hour analysis period. The comparative simulation outcomes indicated that the implementation of DR decreases operating costs from $6,300–$11,150 (corresponding to savings on costs of between $5,500–$15,200) an improvement of between 4.7%–26.6%. The total emissions reduced from 12,825–12,860 kg, amounting to a reduction of 18.3% from the total emissions of between 15,630–15,700kg. The results indicate that DR enhances the coordinated performance of EVs and BESS during peak shaving and load shift applications. Moreover, the utilization of HT enhances the reliability of DR by allocating controllable backup supply when renewable energy is not available. The results indicate that the future of a cost-effective low carbon resilient energy system requires coordinated optimization of distributed resources. The results also broaden the applicability of how grid operators typically view demand response: variable demand and hybrid storage, as a combined, dispersed resource, can offer economic and environmental benefits. Future research should broaden this framework to improve resilience and flexibility in energy systems by exploring multi-microgrid networks, real-time optimization, market-based demand response, and more sophisticated management approaches such as machine learning. Future work will also address large-scale distribution networks with higher numbers of users and additional resources, where runtime growth under increasing system size is to be quantified. Scalability-oriented implementations are to be investigated, including parallel evaluation of candidate solutions and user aggregation into representative profiles, in order to maintain computational tractability for larger systems.

## References

Ahmadi, B., Younesi, S., Ceylan, O., & Ozdemir, A. (2022). An advanced grey wolf optimization algorithm and its application to planning problem in smart grids. *Soft Computing*, 26(8), 3789-3808. https://doi.org/10.1007/s00500-022-06767-9

Ali, A., Shaaban, M. F., & Mahmoud, K. (2024). Optimizing hydrogen systems and demand response for enhanced integration of RES and EVs in smart grids. *IEEE Transactions on Smart Grid*. https://doi.org/10.1109/TSG.2024.3491774

Alzahrani, A., Hafeez, G., Ali, S., Murawwat, S., Khan, M. I., Rehman, K., & Abed, A. M. (2023). Multi-objective energy optimization with load and distributed energy source scheduling in the smart power grid. *Sustainability,* 15(13), 9970. https://doi.org/10.3390/su15139970

Behera, A. P., Chauhan, M., Shrivastava, G., Singh, P., Shukla, J., & Sethi, K. C. (2025). Optimizing trade-off between time, cost, and carbon emissions in construction using NSGA-III: An integrated approach for sustainable development. *Asian Journal of Civil Engineering*, 26(1), 73-87. https://doi.org/10.1007/s42107-024-01176-9

Cerda-Flores, S. C., Rojas-Punzo, A. A., & Nápoles-Rivera, F. (2022). Applications of multi-objective optimization to industrial processes: a literature review. *Processes,* 10(1), 133. https://doi.org/10.3390/pr10010133

Çiçek, A. (2023). Multi-Objective Operation Strategy for a Community with RESs, Fuel Cell EVs and Hydrogen Energy System Considering Demand Response. *Sustainable Energy Technologies and Assessments,* 55, 102957. doi: https://doi.org/10.1016/j.seta.2022.102957

Duan, F., & Bu, X. (2025). A new cloud-stochastic framework for optimized deployment of hydrogen storage in distribution network integrated with renewable energy considering hydrogen-based demand response. *Energy,* 316, 134483. https://doi.org/10.1016/j.energy.2025.134483

Ebrahimi, J., & Abedini, M. (2022). A two-stage framework for demand-side management and energy savings of various buildings in multi smart grid using robust optimization algorithms. *Journal of Building Engineering,* 53, 104486. https://doi.org/10.1016/j.jobe.2022.104486

Güven, A. F., Yörükeren, N., Tag-Eldin, E., & Samy, M. M. (2023). Multi-objective optimization of an islanded green energy system utilizing sophisticated hybrid metaheuristic approach. *IEEe Access*, 11, 103044-103068. https://doi.org/10.1109/ACCESS.2023.3296589

Han, S., Yuan, Y., He, M., Zhao, Z., Xu, B., Chen, D., & Jurasz, J. (2024). A novel day-ahead scheduling model to unlock hydropower flexibility limited by vibration zones in hydropower-variable renewable energy hybrid system. *Applied Energy*, 356, 122379. https://doi.org/10.1016/j.apenergy.2023.122379

He, Y., Guo, S., Zhou, J., Ye, J., Huang, J., Zheng, K., & Du, X. (2022). Multi-objective planning-operation co-optimization of renewable energy system with hybrid energy storages. *Renewable Energy*, 184, 776-790. https://doi.org/10.1016/j.renene.2021.11.116

Hojjatinia, Z., Mezher, A. M., Castillo-Guerra, E., Cardenas-Barrera, J., & Saleh, S. M. A. (2024). Peak shaving impact on load forecasting: A strategy for mitigation. *IEEE Access* .https://doi.org/10.1109/ACCESS.2024.3474569

Holechek, J. L., Geli, H. M. E., Sawalhah, M. N., & Valdez, R. (2022). A global assessment: can renewable energy replace fossil fuels by 2050? *Sustainability,* 14(8), 4792. https://doi.org/10.3390/su14084792

Islam, M. M., Yu, T., Giannoccaro, G., Mi, Y., La Scala, M., Rajabi, M. N., & Wang, J. (2024). Improving reliability and stability of the power systems: A comprehensive review on the role of energy storage systems to enhance flexibility. *IEEE Access,* 12:152738-152765. https://doi.org/10.1109/ACCESS.2024.3476959

Jia, J., Li, H., Wu, D., Guo, J., Jiang, L., & Fan, Z. (2024). Multi-objective optimization study of regional integrated energy systems coupled with renewable energy, energy storage, and inter-station energy sharing. *Renewable Energy*,225,120328. https://doi.org/10.1016/j.renene.2024.120328

Karimi, H., Jadid, S., & Hasanzadeh, S. (2023). Optimal-sustainable multi-energy management of microgrid systems considering integration of renewable energy resources: A multi-layer four-objective optimization. *Sustainable Production and Consumption*, 36, 126-138. https://doi.org/10.1016/j.spc.2022.12.025

Khalil, M., & Sheikh, S. A. (2024). Advancing green energy integration in power systems for enhanced sustainability: A review. *IEEE Access*. https://doi.org/10.1109/ACCESS.2024.3472843

Kheiter, A., Souag, S., Chaouch, A., Boukortt, A., Bekkouche, B., & Guezgouz, M. (2022). Energy management strategy based on marine predators algorithm for grid-connected microgrid. *International Journal of Renewable Energy Development,* 11(3), 751. https://doi.org/10.14710/ijred.2022.42797

Kumar, R. P., & Karthikeyan, G. (2024). A multi-objective optimization solution for distributed generation energy management in microgrids with hybrid energy sources and battery storage system. *Journal of Energy Storage*, 75, 109702. https://doi.org/10.1016/j.est.2023.109702

Lahlou, Y., Hajji, A., & Aggour, M. (2023). Optimization of a Management Algorithm for an Innovative System of Automatic Switching between Two Photovoltaic and Wind Turbine Modes for an Ecological Production of Green Energy. *International Journal of Renewable Energy Development,* 12(1). https://doi.org/10.14710/ijred.2023.47137

Makhadmeh, S. N., Al-Betar, M. A., Doush, I. A., Awadallah, M. A., Kassaymeh, S., Mirjalili, S., & Zitar, R. A. (2023). Recent advances in Grey Wolf Optimizer, its versions and applications. *Ieee Access,* 12, 22991-23028. https://doi.org/10.1109/ACCESS.2023.3304889

Munnaf, M. D., & Islam, T. (2024). Enhancing solar energy prospects: predicting direct normal irradiance in qinghai province using ALO-RF modeling. *Advances in Engineering and Intelligence Systems*, 3(01), 85-98.

Ochoa-Correa, D., Arévalo, P., & Martinez, S. (2025). Pathways to 100% Renewable Energy in Island Systems: A Systematic Review of Challenges, Solutions Strategies, and Success Cases. *Technologies,* 13(5), 180. https://doi.org/10.3390/technologies13050180

Qachchachi, N., Mahmoudi, H., & El Hassnaoui, A. (2020). Control strategy of hybrid AC/DC microgrid in standalone mode. *International Journal of Renewable Energy Development*, 9(2), 295. https://doi.org/10.14710/ijred.9.2.295-301

Qi, J., & Li, L. (2023). Economic operation strategy of an EV parking lot with vehicle-to-grid and renewable energy integration. *Energies,* 16(4), 1793. https://doi.org/10.3390/en16041793

Rabbi, M. F., Popp, J., Máté, D., & Kovács, S. (2022). Energy security and energy transition to achieve carbon neutrality. *Energies,* 15(21), 8126. https://doi.org/10.3390/en15218126

Saeed, M. H., Rana, M. S., Kausaraahmed, M., El-Bayeh, C. Z., & Wang, F. (2023). Demand response based microgrid's economic dispatch. *International Journal of Renewable Energy Development*, 12(4), 749-759. https://doi.org/10.14710/ijred.2023.49165

Saldarini, A., Longo, M., Brenna, M., & Zaninelli, D. (2023). Battery electric storage systems: Advances, challenges, and market trends. Energies, 16(22), 7566. https://doi.org/10.3390/en16227566

Taha, H. A., Alham, M. H., & Youssef, H. K. M. (2022). Multi-objective optimization for optimal allocation and coordination of wind and solar DGs, BESSs and capacitors in presence of demand response. *IEEE Access,* 10, 16225-16241. https://doi.org/10.1109/ACCESS.2022.3149135

Vanlalchhuanawmi, C., Deb, S., Onen, A., & Ustun, T. S. (2024). Energy management strategies in distribution system integrating electric vehicle and battery energy storage system: A review. *Energy Storage*, 6(5), e682. https://doi.org/10.1002/est2.682

Yu, Z., Zheng, W., Zeng, K., Zhao, R., Zhang, Y., & Zeng, M. (2024). Energy optimization management of microgrid using improved soft actor-critic algorithm. *International Journal of Renewable Energy Development,* 13(2), 329-339. https://doi.org/10.61435/ijred.2024.59988

Zhang, G., Ge, Y., Ye, Z., & Al-Bahrani, M. (2023). Multi-objective planning of energy hub on economic aspects and resources with heat and power sources, energizable, electric vehicle and hydrogen storage system due to uncertainties and demand response. *Journal of Energy Storage,* 57, 106160. doi: https://doi.org/10.1016/j.est.2022.106160

Zhang, H. (2024). Application of day-ahead optimal scheduling model based on multi-energy micro-grids with uncertainty in wind and solar energy and energy storage station. *International Journal of Renewable Energy Development,* 13(5), 873-883. https://doi.org/10.61435/ijred.2024.60218

Zhang, Y., Ma, T., Elia Campana, P., Yamaguchi, Y., & Dai, Y. (2020). A techno-economic sizing method for grid-connected household photovoltaic battery systems. *Applied Energy,* 269, 115106. https://doi.org/10.1016/j.apenergy.2020.115106